The Thirteenth International Symposium on Artificial Life and Robotics 2008(AROB 13th '08),
B-Con Plaza, Beppu, Oita, Japan, January 31-February 2, 2008

Cooperative control of multiple neural networks for indoor blimp robot

Ryouta Nishioka , Hidenori Kawamura , Azuma Ohuchi
Toshihiko Takaya , Hiroyuki Iizuka

Graduate School of Information Science and Technology, Hokkaido University
North 14, West 8, Kita-ku, Sapporo, Hokkaido 060-8628, Japan
E-mail : nishioka, kawamura, ohuchi @complex.eng.hokudai.ac.jp
Ricoh Software Inc.
North 7, West 4, Kita-ku, Sapporo, Hokkaido 060-0807, Japan
E-mail : toshihiko.takaya@rsi.ricoh.co.jp
Department of Media Architecture,Future University-Hakodate
116-2 Kamedanakano-cho, Hakodate, Hokkaido, 041-8655, Japan
E-mail : ezca@fun.ac.jp
URL : http://harmo.complex.eng.hokudai.ac.jp/

Abstract

We report on cooperative control of multiple neural networks for indoor blimp robot. In our laboratory, the indoor blimp has been studied to achieve various applications. Our objective of this paper is to propose a robust controller that can adapt to mechanical accidents such as breakdown of propellers. In our proposal method, each propeller thrust is independently calculated by each small network. We confirm effectiveness of the proposed method compared to the method of calculating thrusts by a single large neural network on the simulator.
key words - indoor blimp robot, neural network, cooperative control

1 Introduction

Indoor blimp robot is known as the aerial vehicle. It can move safely in three dimensional space. The advantage is that it consumes lower energy to move than the other aerial vehicles such as helicopters and air planes. Blimp robot can be applied to various applications, for example, guidance in the buildings, monitoring high attitudes and entertainment flight. It has been studied on the speed control, self-charging system and time constraint control[1, 2, 3]. The PID control that is classified as the feedback controls is used in these studies. In the methods, after the thrust of entire robot is calculated, it is distributed to each propeller. However, it is difficult for these methods to adapt to partial breakdowns or environmental changes without tuning by human. As other approaches, it has been studied that the robot movement is emerged and self-organized from individual motor controls through embodiment[4]. Self-organized control can be expected to have robustness against partial breakdowns because the entire control is constructed by interactions among them. The others could make up for partial breakdowns. In this study, breakdowns of propellers are our concern. It is thought that the self-organized method can adapt to the breakdown of the propellers. Therefore we propose a self-organized neural controller implemented in the simulated indoor blimp and compare the effectiveness of the proposed method with the conventional neural network model.

This paper is organized as follows. First, a real blimp robot that we have studied is introduced. In the next section, our proposing method with multiple neural networks is explained. Finally, the effectiveness will be shown.

2 Blimp robot

2.1 Real robot

We designed a cylinder-shaped blimp robot. This shape can greatly take the volume. This blimp robot has three propulsion units, each of which has two propellers in the X, Y, and Z axis. Ch4 worked for vertical movement, and ch0, ch1, ch2 and ch3 are for the X-Y plane. Diameter(D[m]) and Height(H[m]) of the balloon is decided to produce enough to buoyant force. Total weight of blimp robot W[g] is calculated as fol-

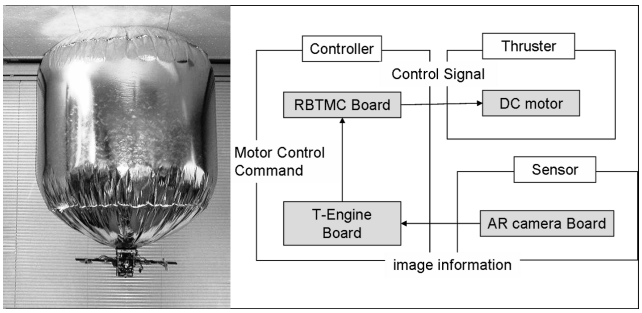

Figure 1: Blimp robot and overview

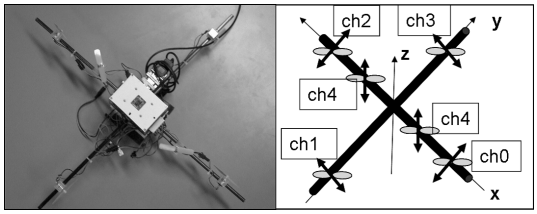

Figure 2: Propeller unit

lows.

$$W = \pi\rho_{he}H(\frac{D}{2})^2 + \pi cD(H + \frac{D}{2}) + U \qquad (1)$$

where $\rho_{he} = 178.5[g/m^3]$ is helium density and, $c[g/m^2]$ is the unit weight of balloon material. Balloon material is aluminum film, whose unit weight c is $30.0[g/m^2]$. U is the weight of the propeller unit that consist of the six propellers, the camera sensor, and the controller. Weight U is about 480[g]. The buoyant force B_u can be calculated by this equation.

$$B_u = \pi\rho_{air}H(\frac{D}{2})^2 \qquad (2)$$

where ρ_{air}=1226.0$[g/m^3]$ at 0 ℃,1atm. B_u must be larger than W. We set diameter D to 0.94[m], and height H to 0.8[m].

The propellers can be driven by only ON/OFF signal.

2.2 Simulator

In our study, we test two types of the neural networks on a simulator that is constructed based on the architecture of the real robot. The air resistance, the buoyancy, and the thrust of the propeller is considered in the equation of motion[5].

We set up the simplest task where the blimp must approach a target in a trial time in order to compare the performances of two neural networks. For the simplicity, we consider only X-Y plane.

3 Neural network

In this section, we describe two types of neural networks to calculate the thrust. One is the method in which each propeller thrust is independently calculated by a small neural network(NNI). Because the characteristic of the propeller is the same, we use the same structure of neural network[6]. Another is the method in which a large neural network decides all blimp thrusts(NNA)(See Fig.3).

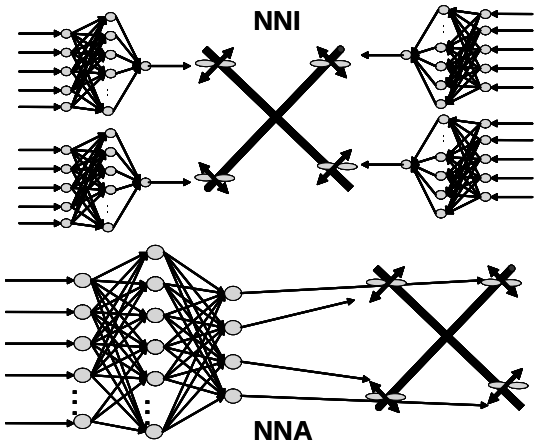

Figure 3: A schematic view of NNI(top) and NNA(bottom)

Input X and the output Z of each small network in NNI are represented as follows.

$$\boldsymbol{X_i^{NNI}(t)}=\{\ Rx_i, Ry_i, Dx_i, Dy_i, z_i(t \quad 1)\ \}$$
$$\boldsymbol{Z_i^{NNI}(t)}=\{\ z_i(t)\ \}$$

where Rx_i and Ry_i is relative positions to the target from each propeller, i. Dx_i and Dy_i are the movements during a time step. The thrust at the previous time step, $z_i(t \quad 1)$ is fed back to the input. $z_i(t)$ is the thrust for a propeller. The inputs for each network are calculated based on the position of propeller 2 as follows.

$$Rx_0 = Ry_1 = Ry_3 = \quad Rx_2$$
$$Ry_0 = Rx_1 = \quad Rx_3 = Ry_2$$

$$
\begin{aligned}
Rx_2 &= tx \quad cos(\ \theta) \quad ty \quad sin(\ \theta) \\
Ry_2 &= tx \quad sin(\ \theta) + ty \quad cos(\ \theta) \\
tx &= T_x \quad X \\
ty &= T_y \quad Y
\end{aligned}
$$

where θ is an angle around Z axis of the blimp. (T_x, T_y) and (X, Y) are positions of the target and the blimp, respectively.

The inputs and outputs of large network in NNA are represented as follows.

$$
\begin{aligned}
\boldsymbol{X^{NNA}(t)}&=\{\ Rx_2, Ry_2, Dx_2, Dy_2, z_0(t \quad 1), z_1(t \\
&\quad 1), z_2(t \quad 1), z_3(t \quad 1)\ \} \\
\boldsymbol{Z^{NNA}(t)}&=\{\ z_0(t), z_1(t), z_2(t), z_3(t)\ \}
\end{aligned}
$$

The inputs of NNA is given by a relative position of propeller number 2. The outputs of NNA are four propeller's thrust.

4 Genetic algorithm

The neural network parameters are evolved by genetic algorithm. One gene consists of parameters of neural networks such as weights and biases as shown in Fig. 4. All genes are evaluated by the distance to the target at the end of trials.

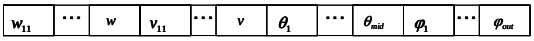

Figure 4: The structure of genes

The fitness function is given as follows.

$$fitness = \frac{1}{T}\sum 1 \quad dist/dist_{init} \tag{3}$$

where T represents the number of trials, and $dist$ and $dist_{init}$ represents distances to the target at the end and at the beginning of the trial, respectively. The fitness is averaged over T(=5) trials starting from different initial positions. These are modified by using crossover and the mutation at every generation. One point crossover was used for the crossover and tournament selection for the selection.

5 Experiment

In this experiment, we confirm the effectiveness of our proposing NNI model compared to NNA. The parameters used by the experiment are shown in Table 1.

Table 1: Parameter of experiment

Parameter	value
Generation	100
Population	100
Tournament size	5
Mutation probability	0.6
Trial time	2000
Target position(X,Y)	(0.5,1)
Initial position of X	[-1.5,1.5]
Initial position of Y	[0,3]

5.1 Result

After being evolved under the all propellers can drive, the both networks have been able to move to the target. To compare robustness of networks acquired in the evolution, we measure the performances when the propellers break down. The average of the fitness over 100 times from a different initial position is shown in Table 2. The table includes the fitness when the all propeller works, one propeller breaks down and two propellers break down. When the propeller breaks down, there is a clear difference of performances between NNI and NNA. Even when the propeller breaks, NNI can mostly approach to the target position. Especially, NNI has a strong robustness to a breakdown of a single propeller. In NNA, the breakdown of a single propeller can cause a serious damage to the controller. Trajectories of all patterns when starting from

Table 2: Fitness to each state

State	propeller number	NNA	NNI
all propeller drive		0.988	0.999
one propeller breaks down	ch0	0.906	0.961
	ch1	-8.050	0.961
	ch2	0.648	0.978
	ch3	-1.072	0.989
two propellers break down	ch0,ch1	0.685	0.752
	ch0,ch2	-2.370	0.521
	ch0,ch3	0.713	0.966
	ch1,ch2	0.515	0.965
	ch1,ch3	-7.409	0.547
	ch2,ch3	-4.591	0.670

the same starting point(-1.0,2.2) are shown in Fig. 5, Fig. 6, and Fig. 7. It should be noted that Fig. 5 has different scale from the others. NNI can keep a

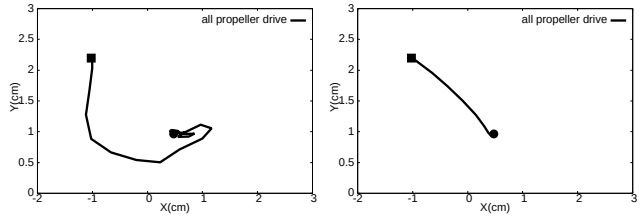

Figure 5: The trajectory of NNA(left) and NNI(right) :all propeller drive

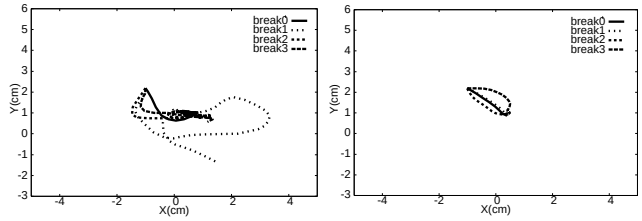

Figure 6: The trajectories of NNA(left) and NNI(right) :one propeller breakdown

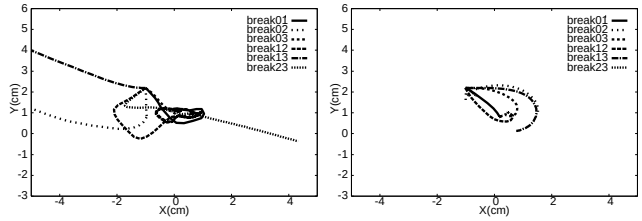

Figure 7: The trajectories of NNA(left) and NNI(right) :two propellers breakdown

similar trajectory even if the propellers break down. On the other hand, NNA cannot approach the target when propellers break down. It can be said that NNI is more robust than NNA in terms of performances and trajectories from these results.

6 Conclusion

We proposed cooperative control of multiple neural networks for indoor blimp control. In this paper, it was shown that the proposed method was more robust to the breakdown of propellers. In future work, task could be more complex to confirm the effectiveness and adaptivity of our proposed method. As another direction, the proposed method will be tested with the real blimp.

Acknowledgments

This research was partially supported by Ricoh Software Inc, PC6A190016.

References

[1] H.Kadota,H.Kawamura,M.Yamamoto, T.Takaya,A.Ohuchi "Vision-Based Motion Control of Indoor Blimp Robot", *Proceedings of The 4th International Conference on Advanced Mechatronics*, 2004

[2] Y.Minagawa,H.Kawamura,M.Yamamoto, T.Takaya,A.Ohuchi "Learning landing control of indoor blimp robot for autonomous energy recharging", *The Twelfth International Symposium on Artificial Life and Robotics*, 2007

[3] H.Kasawaki,H.Kawamura, M.Yamamoto,T.Takaya,A.Ohuchi "Control for Indoor Blimp Robot Based on Flight Plan with Constraint Time(In Japanese)", *Conference on Robotics and Mechatronics*, 2007

[4] Y.Kuniyoshi,S.Suzuki, "Dynamic Emergence and Adaptation of Behavior Through Embodiment as Coupled Chaotic Field", *Intelligent Robots and Systems*, 2004

[5] S.Zwaan,A.Bernardino,Jose Santos Victor "Vision based Station Keeping and Docking for an Aerial Blimp", *International Conference on Intelligent Robots and Systems*,2000

[6] Y.Shim, P.Husbands "Feathered Flyer: Integrating Morphological Computation and Sensory Reflexes into a Physically Simulated Flapping-Wing Robot for Robust Flight Manoeuvre", *European Conference on Artificial Life*, 2007